Composition of Pseudorabies Virus Particles Lacking Tegument Protein US3, UL47, or UL49 or Envelope Glycoprotein E

Kathrin Michael, Barbara G. Klupp, Thomas C. Mettenleiter,* and Axel Karger

*Institute of Molecular Biology, Friedrich-Loeffler-Institut, Boddenblick 5A,
17493 Greifswald-Insel Riems, Germany*

Proteins located in the tegument layer of herpesvirus particles play important roles in the replicative cycle at both early and late times after infection. As major constituents of the virion, they execute important functions in particular during formation of progeny virions. These functions have been mostly elucidated by construction and analysis of mutant viruses deleted in single or multiple tegument protein-encoding genes (reviewed in the work of T. C. Mettenleiter, Virus Res. 106:167–180, 2004). However, since tegument proteins have been shown to be involved in numerous protein-protein interactions, the impact of single protein deletions on the composition of the virus particle is unknown, but they could impair correct interpretation of the results. To analyze how the absence of single virion constituents influences virion composition, we established a procedure to assay relative amounts of virion structural proteins in deletion mutants of the alphaherpesvirus *Pseudorabies virus* (PrV) in comparison to wild-type particles. The assay is based on the mass spectrometric quantitation of virion protein-derived peptides carrying stable isotope mass tags. After deletion of the US3, UL47, UL49, or glycoprotein E gene, relative amounts of a capsid protein (UL38), a capsid-associated protein (UL25), several tegument proteins (UL36 and UL47, if present), and glycoprotein H were unaffected, whereas the content of other tegument proteins (UL46, UL48, and UL49, if present) varied significantly. In the case of the UL48 gene product, a specific increase in incorporation of a smaller isoform was observed after deletion of the UL47 or UL49 gene, whereas a larger isoform remained unaffected. The cellular protein actin was enriched in virions of mutants deficient in any of the tegument proteins UL47, UL49, or US3. By two-dimensional gel electrophoresis multiple isoforms of host cell-derived heat shock protein 70 and annexins A1 and A2 were also identified as structural components of PrV virions.

Pseudorabies virus (PrV) is a member of the *Alphaherpesvirinae* subfamily in the family *Herpesviridae*. Beyond its importance as the causative agent of Aujeszky's disease in pigs (33), it has been widely used as a model for the study of herpesvirus entry and morphogenesis (34, 35). Herpesvirus virions consist of four subviral structural components: the double-stranded genomic DNA in the core is enclosed in an icosahedral capsid which, in turn, is surrounded by a lipid bilayer called the envelope which contains virally encoded glycosylated and non-glycosylated proteins. Between envelope and capsid resides the tegument, which is the most complex structure of the virion, presumably linking the nucleocapsid and the envelope. Of the over 70 genes that were found within the 143-kbp PrV genome, 31 have been shown to code for structural components of the virion. Thirteen of them have been assigned to the tegument layer (24), underlining its importance for the structural and functional integrity of the virion. In keeping with its proposed role in virion formation, a number of interactions between tegument proteins among themselves and with other structural proteins have been described in PrV and other herpesviruses (reviewed in references 33 and 34). Electron microscopic studies of cells infected with mutants deleted in tegument proteins US3 (23), UL11 (27), UL16 (20), UL36 (10), UL37 (21), UL47

(28), UL48 (8), and UL51 (22) have documented the relevance of these tegument proteins for morphogenesis of PrV.

In addition to their structural function, catalytic activity has also been found in tegument proteins. The US3 protein is a protein kinase in PrV (58) and other alphaherpesviruses, e.g., Marek's disease virus (45) and herpes simplex virus type 1 (HSV-1) (7). The UL13 gene product of HSV-1 has also been reported to phosphorylate other viral proteins (42). A deubiquitinating protease activity has been assigned to the HSV-1 UL36 protein (19).

Due to the network of protein-protein interactions involving tegument components, it appears likely that deletion of single tegument proteins may lead to alterations in the overall composition of mutant virus particles beyond the loss of the targeted gene product. Higher amounts of actin were detected in virions of a UL49 deletion mutant of PrV than in wild-type virus particles (4). In the case of a UL20 deletion mutant of PrV, Dietz and coworkers (5) found that the UL53 gene product, glycoprotein K (gK), was not properly processed and localized. Deletion of the US3 gene in HSV-2 led to instability and to drastically decreased incorporation of the UL46 protein into the virus particle (32).

In this study we present a systematic approach to the quantitation of virus structural proteins. Highly purified virion preparations were analyzed by two-dimensional (2D) electrophoresis, and structural components were identified by peptide mass fingerprint analysis. Structural proteins from four PrV mutants deleted in a single gene each were quantified from one-dimensional (1D) gels. A method outlined by Ong and coworkers

* Corresponding author. Mailing address: Friedrich-Loeffler-Institut, Boddenblick 5A, 17493 Greifswald-Insel Riems, Germany. Phone: 49-38351-7250. Fax: 49-38351-7151. E-mail: thomas.mettenleiter@fli.bund.de.

(39) and designated "stable isotope labeling with amino acids in cell culture" (SILAC) was used. The key feature of this procedure is the generation of a global internal standard by metabolic introduction of a stable isotope tag into either sample or reference, whereas the other is cultured under conventional conditions. Samples are then mixed, proteins are separated, and relative amounts of proteins are calculated after tryptic digestion from the intensity ratios of mass-tagged and conventional peaks from the mass spectra. Mutants with single deletions in genes coding for tegument proteins UL47, UL49, and US3 were analyzed, and a gE deletion mutant representing the deletion of a nontegument protein was also included.

MATERIALS AND METHODS

Cells and viruses. PrV mutants deleted in US3 (PrV-ΔUS3) (23), UL47 (PrV-ΔUL47) (28), UL49 (PrV-ΔUL49) (9), and glycoprotein E (PrV-ΔgE) (26) were derived from PrV strain Kaplan (PrV-Ka) (17). They were propagated on porcine kidney cells (Collection of Cell Lines in Veterinary Medicine, Insel Riems, Germany; RIE008). For titrations, 10-fold serial dilutions of virus suspensions were plated onto monolayers of Madin-Darby bovine kidney cells (MDBK cells, supplied by the Collection of Cell Lines in Veterinary Medicine) (31). Inocula were removed after 1 h, and cells were stained with crystal violet after further incubation at 37°C for 48 h.

Purification of pseudorabies virus virions. Twelve cell culture flasks with a 162-cm² growth area of confluent porcine kidney cells were infected at a multiplicity of infection of 1, and cell culture supernatants were harvested between 24 and 30 h after infection. Purification by sucrose gradient centrifugation was performed as described previously (18). Briefly, cellular debris was removed, and virus was purified by sedimentation through a 40% sucrose cushion followed by sucrose density gradient centrifugation. The quality of the virion preparation was verified by electron microscopy.

Stable isotope tagging. The SILAC procedure outlined by Ong and coworkers (39) was adapted. Dulbecco's modified Eagle's medium (DME)–nutrient mixture F12 Ham medium (1:1) (Sigma-Aldrich D-9785) was supplemented with 5% dialyzed fetal calf serum and with all missing amino acids (Sigma-Aldrich) except L-leucine. The medium was then divided and supplemented with either conventional L-leucine (Sigma-Aldrich) or deuterated L-leucine (L-leucine-5,5,5 d₃; Sigma-Aldrich catalog no. 486825; 99 atom% D) to yield Pro-Leu–DME/F-12 or DeuLeu–DME/F-12 cell culture medium, respectively. Porcine kidney cells were passaged in parallel in both media at a 1:6 ratio every 3 days. After four passages samples of the cell cultures were analyzed by sodium dodecyl sulfate (SDS)-polyacrylamide gel electrophoresis, and several protein bands were excised and tryptically digested. The isotope exchange in the deuterated cell batch was then controlled by mass spectrometry. Incorporation of L-leucine-5,5,5 d₃ increases the mass of leucine-containing peptides by 3 mass units per leucine residue. Virus stocks were propagated in porcine kidney cells adapted to ProLeu–DME/F-12 or DeuLeu–DME/F-12. In the latter case, complete exchange of conventional L-leucine with deuterated L-leucine in the virion proteins was ensured by an additional virus passage in porcine kidney cells grown in DeuLeu–DME/F-12.

One-dimensional gel electrophoresis. Samples containing 25 μg each of protonated and deuterated gradient-purified virions were separated in discontinuous SDS-12% polyacrylamide gels using either standard conditions (29) or a bis(2-hydroxyethyl)imino-tris(hydroxymethyl)methane-HCl–2-(N-morpholino) ethanesulfonic acid-buffered electrophoresis system (11) in a Protean II electrophoresis chamber (Bio-Rad, Munich, Germany). For convenience wild-type PrV was labeled with L-leucine-5,5,5 d₃, and the mutants were grown in medium containing conventional L-leucine. After Coomassie blue staining (37) samples were cut out of the centers of the protein bands and processed for peptide mass fingerprint analysis.

Two-dimensional gel electrophoresis. Samples containing 60 μg of purified PrV were sedimented (Beckman TLA45 rotor, 45 min, 45,000 rpm, 4°C) and extracted with rehydration buffer for isoelectric focusing (8 M urea, 2 M thiourea, 1% CHAPS {3-[(3-cholamidopropyl)-dimethylammonio]-1-propanesulfonate}, 20 mM dithiothreitol) (3) by sonication and shaking for 1 h at 20°C. Isoelectric focusing was performed on nonlinear 24-cm IPG strips (Amersham, Braunschweig, Germany) or ReadyStrips (Bio-Rad) in the pH range of 3 to 10 by using an isoelectric focusing cell (Bio-Rad). Thereafter, strips were sequentially equilibrated in buffers containing dithiothreitol and iodoacetamide as rec-

ommended by the manufacturers. For electrophoresis in the second dimension hand-cast 12% acrylamide gels were run in Dodeca Cell or Protean II electrophoresis chambers (Bio-Rad). Gels were fixed and stained overnight with colloidal Coomassie brilliant blue (37). Protein spots of interest were picked as gel plugs of 1.5 mm in diameter.

Peptide mass fingerprints. In-gel tryptic digestion (43) was carried out in 96-well V-bottomed polypropylene microtiter plates with 30 ng trypsin (Promega catalog no. V5111; Mannheim, Germany) per sample for 3 h at 37°C or overnight at 30°C. Mass spectra were registered on a Bruker Ultraflex instrument (Bruker Daltonics, Bremen, Germany) and processed by flexAnalysis 2.0 software (Bruker). For the quantitation of pairs of mass-tagged peptide peaks, it was crucial to choose the SNAP option as peak detection algorithm in the flexAnalysis software, which is robust with respect to overlapping peaks. For database queries following 2D electrophoresis carbamidomethylation was set as fixed modification. In some cases, an additional optional modification allowing a 3-Da mass shift corresponding to an exchange of leucine with deuterated leucine was included. The batch database search (MASCOT Server 2.0.0 software; Matrix Science Ltd., London, United Kingdom) (41) was launched by Biotools 2.2 (Bruker). Proteins were considered identified whenever statistically significant molecular weight search (MOWSE) scores were attained (40) using SwissProt, NCBI, or an in-house database covering the published PrV proteome (24). In some cases, MOWSE scores reached significant levels only after information on leucine content of isotope-labeled peak pairs was added in the query (47).

Quantitation of mass spectrometric data. Evaluation was carried out with an Excel (Microsoft, Redmond, Wash.) spreadsheet. After database search, peaks representing unmodified tryptic peptides of the hit with the highest MOWSE score were selected. The expected masses of the corresponding L-leucine-d₃-labeled peptides were calculated from the leucine content of the peptide. If the calculated masses were found in the peak list within error margins of 50 ppm, the peak pairs were selected for quantitative evaluation. After manual revision mean values of the intensity ratios of all qualified peak pairs representing the identified protein were normalized to the intensity ratio of the 142-kDa form of the UL19 major capsid protein from the same gel. By this normalization step, all protein ratios were referred to the relative content of the major capsid protein in both virus preparations, which reflects the ratio of virus particles, since the number of major capsid protein molecules is 960 for any virus particle (50).

RESULTS

Identification of PrV structural proteins. Proteins from highly purified PrV preparations were resolved by 1D (Fig. 1) or 2D (Fig. 2) electrophoresis and identified by peptide mass fingerprint analysis. Figure 1 shows a representative 1D gel of purified PrV virions indicating the major components of the 24 annotated bands as well as the experimentally derived and calculated molecular weights. In several bands, more than one structural component of PrV was identified, whereas several virion components were found in multiple bands. We did not identify any protein which had not previously been characterized as a structural virion component of PrV or of other alphaherpesviruses (24, 50). On the other hand, our analysis did not resolve all proteins which had been described as components of PrV virions, in particular constituents of the viral envelope. Whereas most of the 27 virally encoded structural proteins that were identified yielded the calculated molecular weight and isoelectric point, several results were noteworthy.

As expected, after 1D electrophoresis the major glycoprotein gB of PrV was detected primarily in three major bands which represent the uncleaved precursor as well as the N-terminal and C-terminal subunits of the disulfide-linked heterodimer (Fig. 1, bands 4, 9, and 11) (15, 30, 54), although gB-related peptides were also observed in adjacent bands possibly due to differential glycosylation resulting in a range of molecular masses. In the 2D gel the larger N-terminal subunit was present in a multitude of spots which most probably represent glycosylation isoforms exhibiting isoelectric points vary-

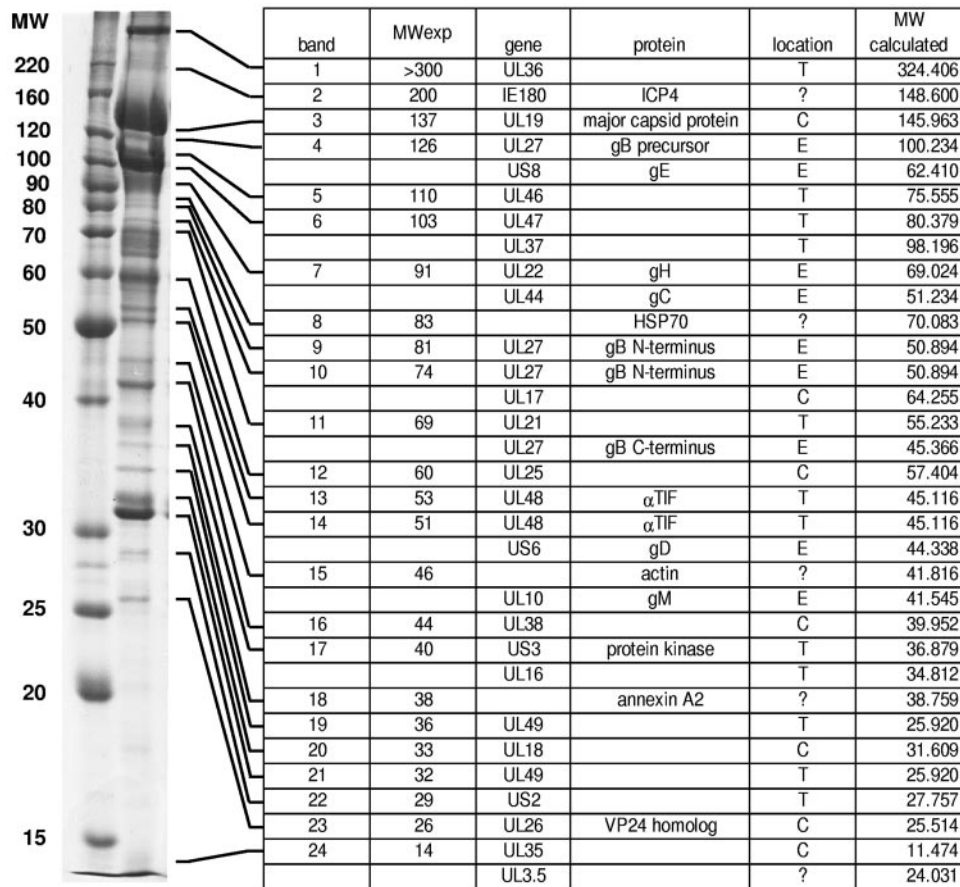| band	MWexp	gene	protein	location	MW calculated
1	>300	UL36		T	324.406
2	200	IE180	ICP4	?	148.600
3	137	UL19	major capsid protein	C	145.963
4	126	UL27	gB precursor	E	100.234
		US8	gE	E	62.410
5	110	UL46		T	75.555
6	103	UL47		T	80.379
		UL37		T	98.196
7	91	UL22	gH	E	69.024
		UL44	gC	E	51.234
8	83		HSP70	?	70.083
9	81	UL27	gB N-terminus	E	50.894
10	74	UL27	gB N-terminus	E	50.894
		UL17		C	64.255
11	69	UL21		T	55.233
		UL27	gB C-terminus	E	45.366
12	60	UL25		C	57.404
13	53	UL48	αTIF	T	45.116
14	51	UL48	αTIF	T	45.116
		US6	gD	E	44.338
15	46		actin	?	41.816
		UL10	gM	E	41.545
16	44	UL38		C	39.952
17	40	US3	protein kinase	T	36.879
		UL16		T	34.812
18	38		annexin A2	?	38.759
19	36	UL49		T	25.920
20	33	UL18		C	31.609
21	32	UL49		T	25.920
22	29	US2		T	27.757
23	26	UL26	VP24 homolog	C	25.514
24	14	UL35		C	11.474
		UL3.5		?	24.031

FIG. 1. Protein profile of purified wild-type PrV-Ka virions after one-dimensional analysis. Protein bands visualized by Coomassie blue staining (left) were numbered from 1 to 24 (first column), and components were identified by peptide mass fingerprint analysis. In several bands, more than one gene product was identified, and several proteins appeared in more than one band. Bands were annotated according to their major component (third column), but the presence of additional components is also indicated. Calculated and observed molecular weights (MW; in thousands) of the gene products (fourth column) are indicated (second and sixth columns). Predicted or confirmed subviral locations of the identified proteins are listed in the fifth column (C = capsid; T = tegument; E = envelope; ? = unclear). All proteins listed here were identified with statistically significant MOWSE scores.

ing from highly acidic to neutral values in a broad range (Fig. 2).

The identified UL26 gene product exhibited a molecular mass below 30 kDa, which is too small considering the calculated molecular mass of 54 kDa for the full-length translation product. In HSV-1 the incorporation into mature virions of only the N-terminal processing product of the UL26 primary translation product designated VP24 has been shown (48). The same apparently applies to the PrV UL26 protein since the tryptic peptides found in virus particles exclusively cover the N-terminal part of UL26.

The UL19 gene product was identified in multiple spots of the expected size of approximately 142 kDa after 2D analysis (Fig. 2). However, in addition seven protein spots which represent C-terminal fragments of 65 to 70 kDa were also found. Charge and/or molecular weight variants have also been observed for the UL18, UL37, and UL48 gene products.

The PrV immediate-early protein 180 (IE180) (16) has been identified in purified virions after 1D electrophoresis (Fig. 1, band 2). For PrV, the presence of this regulatory protein in the virion has not yet been reported, whereas its homolog ICP4 is part of the HSV-1 tegument (57).

In addition to virally encoded components, cellular proteins were also found as structural components of the virion. The presence of actin in the PrV particle (55) was confirmed. We also identified annexins A1 and A2 in PrV virions as well as heat shock protein 70 (HSP70) (Fig. 1 and 2). After 2D electrophoretic separation, three distinct spots were identified as HSP70, and two charge variants each were observed for annexins A1 and A2, respectively. In contrast, actin was represented by one isoform (Fig. 2).

Quantitation of PrV structural components in PrV mutants. To gain insight into the reproducibility of the virus purification procedure and the variation of relative protein contents between virus batches, preparations of mass-tagged and conventional wild-type PrV were mixed and analyzed (Fig. 3). After normalization to the 142-kDa form of the major capsid protein UL19 (MCP142), the relative abundance of all analyzed proteins was close to 1.0, indicating that the purification procedure yielded preparations with very little batch-to-batch variation in
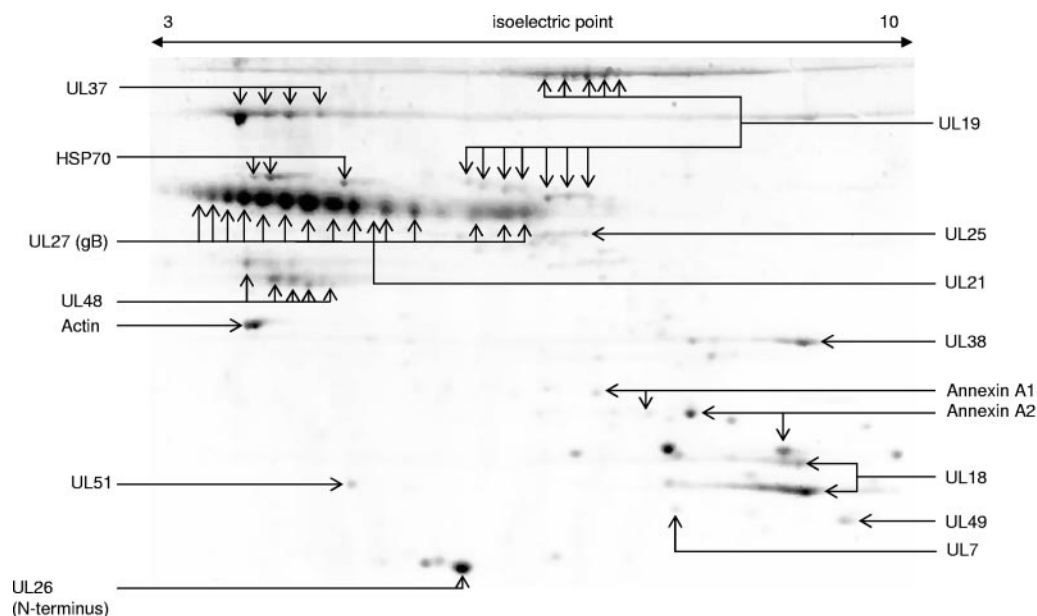
FIG. 2. Proteins from purified wild-type PrV-Ka virions were separated by two-dimensional electrophoresis, and the resulting protein spots were identified by peptide mass fingerprint analysis. Isoelectric focusing strips were used in the nonlinear gradient range of pH 3 to 10. A number of proteins were found in multiple size and/or charge modifications. Note that isoelectric points of gB isoforms vary from values close to 3 to up to 7. The UL48 protein appears in two horizontal chains of charge variants corresponding to bands 13 and 14 from the one-dimensional analysis (Fig. 1).

relative protein content. Margins of error which indicate the variation of the intensity ratios of the peptides used for quantitation rarely exceeded 15%.

In Fig. 4 data on the relative amounts of structural proteins located in or associated with the capsid (UL25 and UL38), tegument (UL36, UL46, UL47, UL48, UL49, and actin) or envelope (UL22/gH) are summarized. The results were obtained by analyses of two independent virus preparations (black or white bars) of PrV-ΔUS3, PrV-ΔUL47, PrV-ΔUL49, or PrV-ΔgE compared with mass-tagged wild-type PrV-Ka. Proteins to be analyzed were selected on the basis of an unambiguous identification in 1D gels and satisfactory data acquisition. In Fig. 4A, proteins are summarized which do not show quantitative variation in the mutant viruses. This had been expected for the capsid protein UL38 but was also found for the capsid-associated UL25 protein and tegument proteins UL36 and UL47 (if present). Glycoprotein H, the UL22 gene product, was also incorporated into virions in constant amounts (Fig. 4A). In contrast, variation of the other identified glycoproteins gB, gC, gD, and gE among preparations was so extensive that no consistent data could be acquired.

In contrast, the relative quantities of proteins represented in Fig. 4B changed drastically upon deletion of other proteins. Deletion of any of the tegument proteins US3, UL47, and UL49, but not deletion of glycoprotein E, led to a striking accumulation of actin which had previously been reported only for a UL49 deletion mutant of PrV (4). In fact, incorporation of actin was even more pronounced in the absence of UL47, resulting in a 5- to 10-fold increase in the virus particle. A decrease of tegument protein UL46 was observed after deletion of US3, which parallels an observed instability and decreased incorporation of the UL46 protein into HSV-2 parti-

cles in the absence of the US3 protein (32). Deletion of gE was accompanied by a marked decrease of UL49 content, which could be explained by the interaction of these two proteins (9).

In Fig. 4C, a differential effect of the deletion of UL47 or UL49 on the relative quantities of the two identified isoforms of the UL48 protein is demonstrated. Whereas the smaller isoform present in band 14 (Fig. 1) accumulated significantly, the amount of UL48 in band 13 remained constant.

DISCUSSION

A common strategy for elucidating the function of viral proteins is the construction and analysis of specific deletion mutants and corresponding rescuant viruses. However, the correct interpretation of the data and the assignment of a specific function to a specific viral gene product often rely on the assumption that the absence of a single protein does not impair any other viral function in *trans*. This is particularly relevant in studies of virion morphogenesis since virion formation in the herpesviruses entails a complex network of protein-protein interactions which are only incompletely understood (34, 35, 53). In this paper, we analyzed wild-type PrV virions by 1D and 2D electrophoresis and devised a strategy for exact relative quantitation of structural components of PrV particles using selective protein label with mass-tagged leucine.

By 1D electrophoresis 24 major protein bands derived from purified virions were identified which, by mass spectrometry, could be annotated to 25 different viral gene products. All of them had previously been characterized as structural components of virions of PrV or of other alphaherpesviruses (24, 50). We are aware that our analysis did not identify all virion constituents and that, in particular, viral envelope proteins
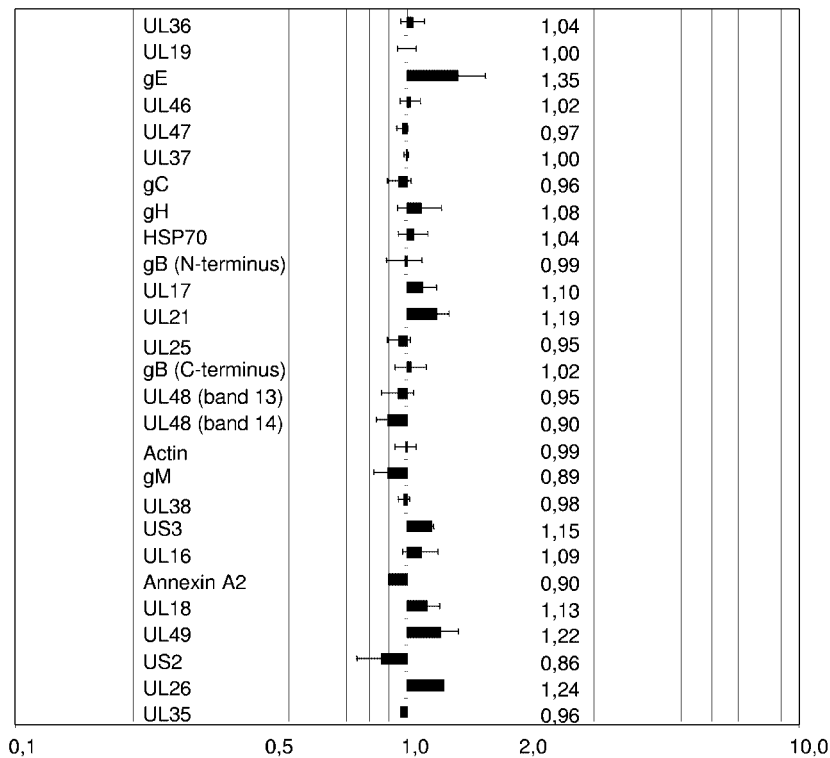
FIG. 3. Structural proteins from two independent preparations of wild-type PrV-Ka were quantitated as described in Materials and Methods. After normalization to the UL19 gene product MCP142, values for all identified proteins were near 1.0, indicating that the purification procedure is reliable. Numbers indicate the relative abundances of the respective proteins in the mass-tagged PrV-Ka preparation compared to the untagged preparation. Error bars indicate the variation of the intensity ratios of the peptides used for the quantitation.

were not adequately represented. By alterations in the gel systems this could possibly be overcome, if desired. Whereas most of the identified proteins exhibited the expected molecular weight and isoelectric points calculated from their primary amino acid sequence, variations did occur.

Perhaps most strikingly, the major glycoprotein B, which, after 1D separation, was identified as the uncleaved precursor as well as the amino- and carboxy-terminal cleavage products (15, 30, 54), produced a multitude of spots after 2D electrophoresis. They could all be assigned to the amino-terminal subunit and most likely represent glycosylation isoforms. The biological relevance of this striking variance resulting in isoelectric points between pH 3 and 7 is unclear at present. Differentially charged variants of glycoproteins gB, gC, and gD which were shown to be modified by sialic acid have also been found after infection of BHK cells with HSV-1 (14).

The major capsid protein UL19 also exhibited multiple isoforms after 2D electrophoresis (Fig. 2) which have not been described so far. Moreover, besides the 142-kDa form of the protein, seven protein spots which represent C-terminal fragments of 65 to 70 kDa were also identified. So far it is unclear whether these fragments were formed during the analytic process or are indeed present in the virion and serve a function there. Charge isoforms were also observed for the UL18, UL37, and UL48 gene products.

The incorporation of cellular proteins into viral particles is rather common. Actin has been detected in a number of other enveloped viruses, such as human immunodeficiency virus (1),

human respiratory syncytial virus (51), or rabies virus (36), and actin-like filaments have been found located at the outer rim of the tegument in the vicinity of the viral envelope in a cryo-electron tomographic reconstruction of the HSV-1 particle (12). Actin has also previously been detected in PrV (55). By 2D analysis we also identified annexins A1 and A2 as constituents of purified PrV virions. The presence of annexins in herpesvirus particles has been observed before (52, 56), which in the light of their capacity to bind both actin and phospholipids is not surprising since both are present in herpesvirus virions. We also detected heat shock protein 70 in PrV virions, which was identified in three distinct spots after 2D gel electrophoresis. Due to the high homology between the highly inducible HSP70 and the constitutively expressed HSC70 protein, we were not able to reliably differentiate between these two proteins. Both are related to the life cycle of alphaherpesviruses as they are recruited into the nucleus after infection with HSV-1 (2). Kobayashi and coworkers (25) reported a drastic upregulation of HSP70 after infection with HSV-1 or HSV-2, but so far there has been no evidence for the incorporation of this protein into herpes simplex virus virions. In contrast, HSP70 has been reported as a structural component of human cytomegalovirus (52), rabies virus (44), and primate lentiviruses (13).

For exact quantitative comparison between wild-type and mutant PrV particles we used the SILAC technique. This procedure conveniently allows the quantitation of virus and host cell-derived structural components of purified virus particles
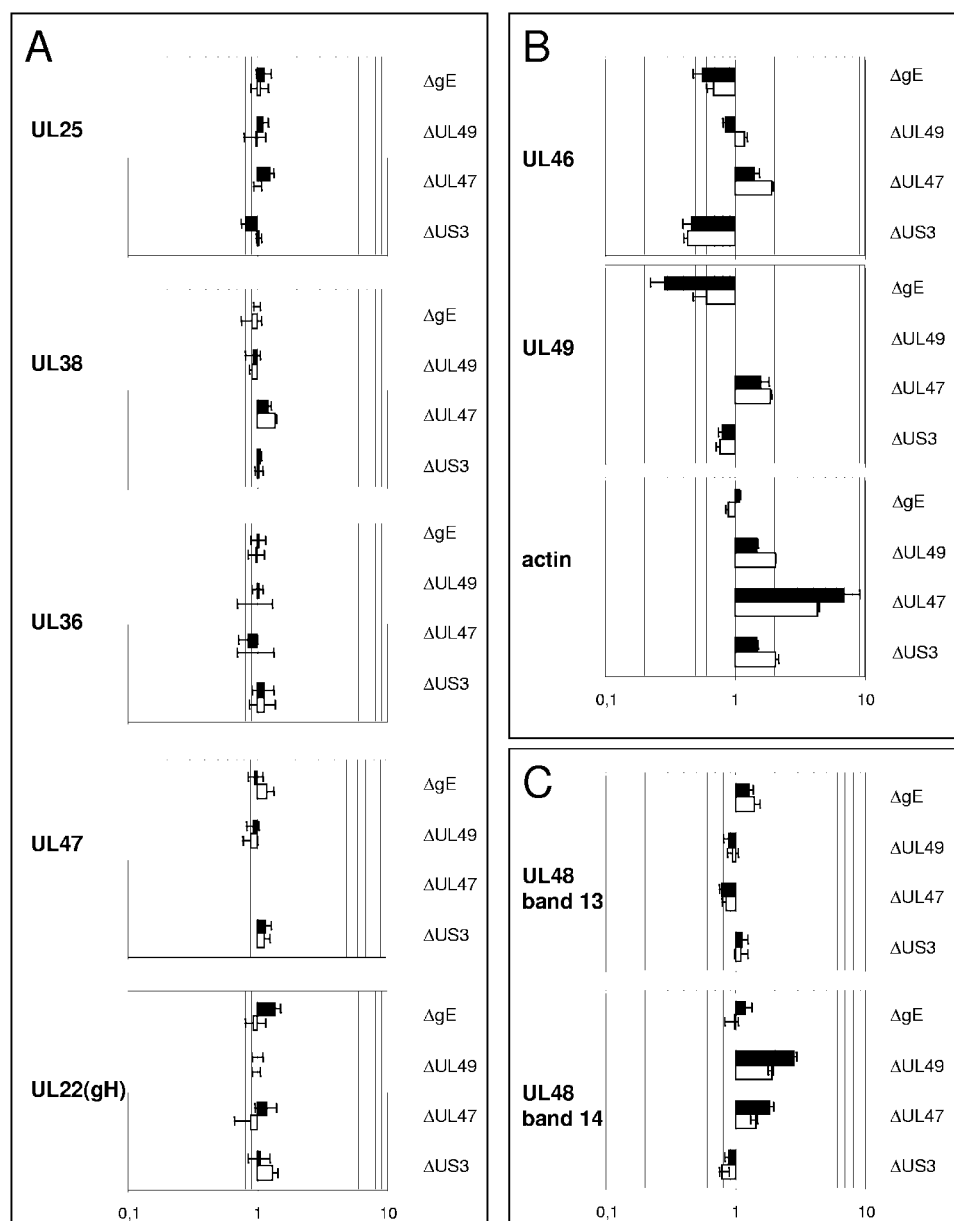
FIG. 4. Relative abundances of structural proteins in PrV mutants compared to wild-type PrV-Ka. Black and white bars represent two independent experiments. Error bars indicate the variation of the intensity ratios of the peptides from one spectrum selected for quantitation. Deleted genes are indicated on the right; the identity of the quantitated protein is given on the left. (A) Proteins with no significant changes in relative abundances after deletion of the US3, UL47, UL49, or gE genes. (B) Proteins that exhibit variations upon deletion of gE, UL49, UL47, or US3. (C) Differential effects on incorporation of two isoforms of UL48 are documented. After deletion of UL47 or UL49, the relative content of UL48 in the lower-molecular-weight band 14 (Fig. 1) increased, whereas the higher-molecular-weight form of UL48 present in band 13 remained stable.

independent of immunological reagents. The use of a global internal standard abolishes the influence of gel-to-gel variations, and in addition to the classical SILAC approach, the subsequent normalization to the 142-kDa major capsid protein encoded by the UL19 gene corrects for any variations in the amount of input virus. Taken together, this led to a very low variance in the measurement of relative protein contents so that even minor changes could be detected. Since data were selected from peptides reliably representing the protein to be evaluated, any disturbing background which is often present after 1D electrophoresis was reduced to a minimum. This

allowed us to choose 1D electrophoretic gels as a starting point for the quantitation, taking into account the higher solubility of most proteins in SDS-containing sample buffer compared to the rehydration buffer used for first-dimension isoelectric focusing. The presence of more than one protein species in one band did not seriously impair identification or quantitation of a specific protein. Nevertheless, 2D analysis has been shown to be useful and two structural proteins (UL7 and UL51) could not be identified from 1D separations but were identified only after 2D electrophoresis.

The comparison of different batches of purified wild-type

PrV virions by the SILAC procedure demonstrated its superb reproducibility. The variation in the incorporation of a multitude of viral and the several identified cellular proteins was minor, and relative amounts of these proteins stayed close to 1.0 (Fig. 3). Thus, there was only little batch-to-batch variation, which provided the basis for subsequent analyses comparing wild-type and mutant viruses for their protein content.

To this end we analyzed PrV mutants lacking the tegument protein US3, UL47, or UL49 or glycoprotein gE for alterations in protein composition of viral particles. Using this novel approach, we were able to confirm the increased incorporation into PrV particles of actin in the absence of UL49 (4). In the absence of US3, UL46 incorporation decreased, which parallels data from HSV-2 in which deletion of US3 resulted in a concomitant loss of the UL46 protein due to instability (32). However, we did not assay whether the decrease of UL46 incorporation in the PrV US3 deletion mutant results from instability of the UL46 protein or is due solely to less efficient packaging of the protein into progeny virions. Together, these results were reassuring since they served to validate our approach. Interestingly, an accumulation of actin was also detected after deletion of US3 or UL47 but not after deletion of glycoprotein E. In fact, incorporation of actin was even more increased in the absence of UL47 than in the absence of UL49, whereas lack of US3 resulted in a similar level of actin incorporation as lack of UL49 did. However, an indirect effect of the US3 deletion on actin incorporation by reduction of the incorporation of the UL46 protein could not be excluded. These data may suggest that the tegument is replenished to a critical volume by cellular actin whenever the major viral component UL46, UL47, or UL49 is decreased or absent (4).

The decrease in the level of UL49 protein in PrV-ΔgE virions is in line with our previous observation that UL49 and gE interact. Thus, the presence of gE might support the recruitment of UL49 into the virion during morphogenesis, whereas UL49 is not required for incorporation of gE (9). We have previously shown that the PrV UL49 protein also interacts with gM and that deletion of both gE and gM resulted in a complete lack of UL49 incorporation (9). Thus, the residual amount of UL49 present in the gE deletion mutant might be recruited via gM. Again, the finding that UL49 incorporation is decreased in the absence of only gE demonstrates the power of our assay system.

Particularly striking was the result that not only the bona fide capsid protein UL38 and the capsid-associated UL25 but also components of the inner tegument, UL36, and the proposed outer tegument, UL47, remain unaffected by the deletion of US3, UL47, UL49, or gE. Moreover, gH was also present in invariant amounts in all the different virus mutants tested. Thus, there appears to be a strict molecular stoichiometry of these proteins in the virus particle which is independent of the other tegument and envelope components tested. This is not true for other envelope proteins such as gB, gC, gD, or gE, whose amount in virions varies extensively even between different batches of wild-type virus (data not shown). Therefore, in future experiments targeting specifically the envelope of mature virions, e.g., for analysis of the movement of glycoprotein-containing virions or vesicles, the visualization of gH might provide a more accurate picture than the observation of other virally encoded glycoproteins.

After two-dimensional electrophoresis (Fig. 4) bands 13 and 14 of 1D electrophoretic separations have been shown to be composed of a multitude of spots that are derived from the UL48 protein. The charge variants found within band 14 most probably represent different levels of phosphorylation which have been found in the UL48 homolog of HSV-1, the VP16 protein (38). Whereas the higher-molecular-weight species of UL48 (band 13) was present in invariant amounts in all mutant viruses tested, the lower-molecular-weight form of the protein (band 14) was specifically enriched in mutant viruses lacking UL49 or UL47. Further analyses will show if the observed compensation of the UL47 or UL49 proteins by UL48 protein is specific for single isoforms appearing in band 14. Thus, we found a differential regulation of incorporation of UL48 gene products into the PrV virion. The UL48 protein of HSV-1 has been demonstrated to physically interact with the UL36, UL41, UL46, UL47, and UL49 tegument proteins (6, 46, 49, 53). From our data it can be deduced that at least two different forms of the PrV UL48 protein exist which are differentially affected by mutations influencing virion composition. It would be interesting to analyze whether two different isoforms of the UL48 protein are also formed during HSV-1 infection and whether at least a part of the observed interactions may be isoform specific.

Finally, our approach for exact quantitation of virion constituents should be generally applicable to any other virus that can be propagated and isotope labeled in cell culture and highly purified in sufficient amounts and that contains a protein suitable for calibration. Thus, this method could become standard in the exact molecular analysis and comparison of virus particles derived from different parental strains, isolates, or mutants.

REFERENCES

1. **Arthur, L. O., J. W. Bess, Jr., R. C. Sowder, R. E. Benveniste, D. L. Mann, J. C. Chermann, and L. E. Henderson.** 1992. Cellular proteins bound to immunodeficiency viruses: implications for pathogenesis and vaccines. Science **258:**1935–1938.
2. **Burch, A. D., and S. K. Weller.** 2004. Nuclear sequestration of cellular chaperone and proteasomal machinery during herpes simplex virus type 1 infection. J. Virol. **78:**7175–7185.
3. **Büttner, K., J. Bernhardt, C. Scharf, R. Schmid, U. Mader, C. Eymann, H. Antelmann, A. Volker, U. Volker, and M. Hecker.** 2001. A comprehensive two-dimensional map of cytosolic proteins of *Bacillus subtilis*. Electrophoresis **22:**2908–2935.
4. **del Rio, T., C. J. Decoste, and L. W. Enquist.** 2005. Actin is a component of the compensation mechanism in pseudorabies virus virions lacking the major tegument protein VP22. J. Virol. **79:**8614–8619.
5. **Dietz, P., B. G. Klupp, W. Fuchs, B. Köllner, E. Weiland, and T. C. Mettenleiter.** 2000. Pseudorabies virus glycoprotein K requires the UL20 gene product for processing. J. Virol. **74:**5083–5090.
6. **Elliott, G., G. Mouzakitis, and P. O'Hare.** 1995. VP16 interacts via its activation domain with VP22, a tegument protein of herpes simplex virus, and is relocated to a novel macromolecular assembly in coexpressing cells. J. Virol. **69:**7932–7941.
7. **Frame, M. C., F. C. Purves, D. J. McGeoch, H. S. Marsden, and D. P. Leader.** 1987. Identification of the herpes simplex virus protein kinase as the product of viral gene US3. J. Gen. Virol. **68:**2699–2704.
8. **Fuchs, W., H. Granzow, B. G. Klupp, M. Kopp, and T. C. Mettenleiter.** 2002. The UL48 tegument protein of pseudorabies virus is critical for intracytoplasmic assembly of infectious virions. J. Virol. **76:**6729–6742.
9. **Fuchs, W., B. G. Klupp, H. Granzow, C. Hengartner, A. Brack, A. Mundt, L. W. Enquist, and T. C. Mettenleiter.** 2002. Physical interaction between

envelope glycoproteins E and M of pseudorabies virus and the major tegu-
ment protein UL49. J. Virol. **76:**8208–8217.

10. **Fuchs, W., B. G. Klupp, H. Granzow, and T. C. Mettenleiter.** 2004. Essential
function of the pseudorabies virus UL36 gene product is independent of its
interaction with the UL37 protein. J. Virol. **78:**11879–11889.

11. **Graham, D. R., C. P. Garnham, Q. Fu, J. Robbins, and J. E. Van Eyk.** 2005.
Improvements in two-dimensional gel electrophoresis by utilizing a low cost
"in-house" neutral pH sodium dodecyl sulfate-polyacrylamide gel electro-
phoresis system. Proteomics **5:**2309–2314.

12. **Grünewald, K., P. Desai, D. C. Winkler, J. B. Heymann, D. M. Belnap, W.
Baumeister, and A. C. Steven.** 2003. Three-dimensional structure of herpes
simplex virus from cryo-electron tomography. Science **302:**1396–1398.

13. **Gurer, C., A. Cimarelli, and J. Luban.** 2002. Specific incorporation of heat
shock protein 70 family members into primate lentiviral virions. J. Virol.
76:4666–4670.

14. **Haarr, L., and H. S. Marsden.** 1981. Two-dimensional gel analysis of HSV
type 1-induced polypeptides and glycoprotein processing. J. Gen. Virol.
52:77–92.

15. **Hampl, H., T. Ben Porat, L. Ehrlicher, K. O. Habermehl, and A. S. Kaplan.**
1984. Characterization of the envelope proteins of pseudorabies virus. J. Vi-
rol. **52:**583–590.

16. **Ihara, S., L. Feldman, S. Watanabe, and T. Ben Porat.** 1983. Characteriza-
tion of the immediate-early functions of pseudorabies virus. Virology **131:**
437–454.

17. **Kaplan, A. S., and A. E. Vatter.** 1959. A comparison of herpes simplex and
pseudorabies viruses. Virology **7:**394–407.

18. **Karger, A., B. Bettin, H. Granzow, and T. C. Mettenleiter.** 1998. Simple and
rapid purification of alphaherpesviruses by chromatography on a cation
exchange membrane. J. Virol. Methods **70:**219–224.

19. **Kattenhorn, L. M., G. A. Korbel, B. M. Kessler, E. Spooner, and H. L.
Ploegh.** 2005. A deubiquitinating enzyme encoded by HSV-1 belongs to a
family of cysteine proteases that is conserved across the family Herpesviri-
dae. Mol. Cell **19:**547–557.

20. **Klupp, B. G., S. Böttcher, H. Granzow, M. Kopp, and T. C. Mettenleiter.**
2005. Complex formation between the UL16 and UL21 tegument proteins of
pseudorabies virus. J. Virol. **79:**1510–1522.

21. **Klupp, B. G., W. Fuchs, H. Granzow, R. Nixdorf, and T. C. Mettenleiter.**
2002. Pseudorabies virus UL36 tegument protein physically interacts with the
UL37 protein. J. Virol. **76:**3065–3071.

22. **Klupp, B. G., H. Granzow, R. Klopfleisch, W. Fuchs, M. Kopp, M. Lenk, and
T. C. Mettenleiter.** 2005. Functional analysis of the pseudorabies virus UL51
protein. J. Virol. **79:**3831–3840.

23. **Klupp, B. G., H. Granzow, and T. C. Mettenleiter.** 2001. Effect of the
pseudorabies virus US3 protein on nuclear membrane localization of the
UL34 protein and virus egress from the nucleus. J. Gen. Virol. **82:**2363–2371.

24. **Klupp, B. G., C. J. Hengartner, T. C. Mettenleiter, and L. W. Enquist.** 2004.
Complete, annotated sequence of the pseudorabies virus genome. J. Virol.
78:424–440.

25. **Kobayashi, K., E. Ohgitani, Y. Tanaka, M. Kita, and J. Imanishi.** 1994.
Herpes simplex virus-induced expression of 70 kDa heat shock protein
(HSP70) requires early protein synthesis but not viral DNA replication.
Microbiol. Immunol. **38:**321–325.

26. **Kopp, M., H. Granzow, W. Fuchs, B. Klupp, and T. C. Mettenleiter.** 2004.
Simultaneous deletion of pseudorabies virus tegument protein UL11 and
glycoprotein M severely impairs secondary envelopment. J. Virol. **78:**3024–
3034.

27. **Kopp, M., H. Granzow, W. Fuchs, B. G. Klupp, E. Mundt, A. Karger, and
T. C. Mettenleiter.** 2003. The pseudorabies virus UL11 protein is a virion
component involved in secondary envelopment in the cytoplasm. J. Virol.
77:5339–5351.

28. **Kopp, M., B. G. Klupp, H. Granzow, W. Fuchs, and T. C. Mettenleiter.** 2002.
Identification and characterization of the pseudorabies virus tegument pro-
teins UL46 and UL47: role for UL47 in virion morphogenesis in the cyto-
plasm. J. Virol. **76:**8820–8833.

29. **Laemmli, U. K.** 1970. Cleavage of structural proteins during the assembly of
the head of bacteriophage T4. Nature **227:**680–685.

30. **Lukacs, N., H. J. Thiel, T. C. Mettenleiter, and H. J. Rziha.** 1985. Demon-
stration of three major species of pseudorabies virus glycoproteins and iden-
tification of a disulfide-linked glycoprotein complex. J. Virol. **53:**166–173.

31. **Madin, S. H., and N. B. Darby, Jr.** 1958. Established kidney cell lines of
normal adult bovine and ovine origin. Proc. Soc. Exp. Biol. Med. **98:**574–576.

32. **Matsuzaki, A., Y. Yamauchi, A. Kato, F. Goshima, Y. Kawaguchi, T. Yo-
shikawa, and Y. Nishiyama.** 2005. US3 protein kinase of herpes simplex virus
type 2 is required for the stability of the UL46-encoded tegument protein
and its association with virus particles. J. Virol. **86:**1979–1985.

33. **Mettenleiter, T. C.** 2000. Aujeszky's disease (pseudorabies) virus: the virus
and molecular pathogenesis—state of the art, June 1999. Vet. Res. **31:**99–
115.

34. **Mettenleiter, T. C.** 2002. Herpesvirus assembly and egress. J. Virol. **76:**1537–
1547.

35. **Mettenleiter, T. C.** 2004. Budding events in herpesvirus morphogenesis.
Virus Res. **106:**167–180.

36. **Naito, S., and S. Matsumoto.** 1978. Identification of cellular actin within the
rabies virus. Virology **91:**151–163.

37. **Neuhoff, V., N. Arold, D. Taube, and W. Ehrhardt.** 1988. Improved staining
of proteins in polyacrylamide gels including isoelectric focusing gels with
clear background at nanogram sensitivity using Coomassie Brilliant Blue
G-250 and R-250. Electrophoresis **9:**255–262.

38. **O'Reilly, D., O. Hanscombe, and P. O'Hare.** 1997. A single serine residue at
position 375 of VP16 is critical for complex assembly with Oct-1 and HCF
and is a target of phosphorylation by casein kinase II. EMBO J. **16:**2420–
2430.

39. **Ong, S. E., B. Blagoev, I. Kratchmarova, D. B. Kristensen, H. Steen, A.
Pandey, and M. Mann.** 2002. Stable isotope labeling by amino acids in cell
culture, SILAC, as a simple and accurate approach to expression proteomics.
Mol. Cell Proteomics **1:**376–386.

40. **Pappin, D. J., P. Hojrup, and A. J. Bleasby.** 1993. Rapid identification of
proteins by peptide-mass fingerprinting. Curr. Biol. **3:**327–332.

41. **Perkins, D. N., D. J. Pappin, D. M. Creasy, and J. S. Cottrell.** 1999. Prob-
ability-based protein identification by searching sequence databases using
mass spectrometry data. Electrophoresis **20:**3551–3567.

42. **Purves, F. C., and B. Roizman.** 1992. The UL13 gene of herpes simplex virus
1 encodes the functions for posttranslational processing associated with
phosphorylation of the regulatory protein alpha 22. Proc. Natl. Acad. Sci.
USA **89:**7310–7314.

43. **Rosenfeld, J., J. Capdevielle, J. C. Guillemot, and P. Ferrara.** 1992. In-gel
digestion of proteins for internal sequence analysis after one- or two-dimen-
sional gel electrophoresis. Anal. Biochem. **203:**173–179.

44. **Sagara, J., and A. Kawai.** 1992. Identification of heat shock protein 70 in the
rabies virion. Virology **190:**845–848.

45. **Sakaguchi, M., T. Urakawa, Y. Hirayama, N. Miki, M. Yamamoto, G. S. Zhu,
and K. Hirai.** 1993. Marek's disease virus protein kinase gene identified
within the short unique region of the viral genome is not essential for viral
replication in cell culture and vaccine-induced immunity in chickens. Virol-
ogy **195:**140–148.

46. **Schmelter, J., J. Knez, J. R. Smiley, and J. P. Capone.** 1996. Identification
and characterization of a small modular domain in the herpes simplex virus
host shutoff protein sufficient for interaction with VP16. J. Virol. **70:**2124–
2131.

47. **Sechi, S., and B. T. Chait.** 2000. A method to define the carboxyl terminal of
proteins. Anal. Chem. **72:**3374–3378.

48. **Sheaffer, A. K., W. W. Newcomb, J. C. Brown, M. Gao, S. K. Weller, and D. J.
Tenney.** 2000. Evidence for controlled incorporation of herpes simplex virus
type 1 UL26 protease into capsids. J. Virol. **74:**6838–6848.

49. **Smibert, C. A., B. Popova, P. Xiao, J. P. Capone, and J. R. Smiley.** 1994.
Herpes simplex virus VP16 forms a complex with the virion host shutoff
protein vhs. J. Virol. **68:**2339–2346.

50. **Steven, A. C., and P. G. Spear.** 1997. Herpesvirus capsid assembly and
envelopment, p. 312–351. *In* W. Chiu, W. M. Burnett, and R. Garcea (ed.),
Structural biology of viruses. Oxford University Press, New York, N.Y.

51. **Ulloa, L., R. Serra, A. Asenjo, and N. Villanueva.** 1998. Interactions between
cellular actin and human respiratory syncytial virus (HRSV). Virus Res.
53:13–25.

52. **Varnum, S. M., D. N. Streblow, M. E. Monroe, P. Smith, K. J. Auberry, L.
Pasa-Tolic, D. Wang, D. G. Camp, K. Rodland, S. Wiley, W. Britt, T. Shenk,
R. D. Smith, and J. A. Nelson.** 2004. Identification of proteins in human
cytomegalovirus (HCMV) particles: the HCMV proteome. J. Virol.
78:10960–10966.

53. **Vittone, V., E. Diefenbach, D. Triffett, M. W. Douglas, A. L. Cunningham,
and R. J. Diefenbach.** 2005. Determination of interactions between tegument
proteins of herpes simplex virus type 1. J. Virol. **79:**9566–9571.

54. **Wolfer, U., V. Kruft, D. Sawitzky, H. Hampl, B. Wittmann-Liebold, and
K. O. Habermehl.** 1990. Processing of pseudorabies virus glycoprotein gII.
J. Virol. **64:**3122–3125.

55. **Wong, M. L., and C. H. Chen.** 1998. Evidence for the internal location of
actin in the pseudorabies virion. Virus Res. **56:**191–197.

56. **Wright, J. F., A. Kurosky, E. L. Pryzdial, and S. Wasi.** 1995. Host cellular
annexin II is associated with cytomegalovirus particles isolated from cultured
human fibroblasts. J. Virol. **69:**4784–4791.

57. **Yao, F., and P. A. Schaffer.** 1994. Physical interaction between the herpes
simplex virus type 1 immediate-early regulatory proteins ICP0 and ICP4.
J. Virol. **68:**8158–8168.

58. **Zhang, G., R. Stevens, and D. P. Leader.** 1990. The protein kinase encoded
in the short unique region of pseudorabies virus: description of the gene and
identification of its product in virions and in infected cells. J. Gen. Virol.
71:1757–1765.

Vol. 80, No. 3

SPOTLIGHT

Articles of Significant Interest Selected from This Issue by the Editors

High-Resolution Molecular and Antigenic Structure Suggests Differences in the Spikes of Virulent Human Rotavirus Strains

To date, only rotavirus strains that attach to cells when their spikes bind sialosides have been analyzed structurally. Rotaviruses that cause human disease do not bind sialosides. Monnier et al. (p. 1513–1523) determined the crystal structure of spike heads from a virulent human rotavirus strain and mapped neutralization escape mutations selected by human monoclonal antibodies. The structure shows a disrupted sialoside-binding site and suggests an alternative ligand-binding region. Antigenic mapping and comparison to an electron cryomicroscopy image reconstruction of virions indicate that the surfaces and spike morphologies recognized by neutralizing antibodies differ between sialoside-dependent and sialoside-independent rotaviruses.

A Molecular Switch for Paramyxovirus Receptor-Binding Activity

The receptor-binding protein (hemagglutinin-neuraminidase, HN) of the paramyxovirus Newcastle disease virus (NDV) has two binding sites, only one of which has receptor-cleaving activity. Porotto et al. (p. 1204–1213) show that engagement of the first receptor-binding site by molecules that mimic the receptor leads to activation of the second binding site. The results provide a possible explanation for how the two disparate activities of a paramyxovirus HN molecule are regulated during infection; the second site may be activated upon attachment to the target cell, but shut off after budding. This work suggests new antiviral strategies that take advantage of the interdependence of the two binding sites.

Receptors for BK Virus

The BK polyomavirus is an emerging concern in the field of transplantation medicine. Advances in immunosuppression have led to BK virus reactivation in increasing numbers of bone marrow and kidney transplant recipients. Low et. al. (p. 1361–1366) demonstrate that the gangliosides GD1b and GT1b are receptors for the virus and that disruption of endoplasmic reticulum trafficking inhibits infection. The identification of gangliosides as receptors for BK virus, as well as the characterization of an additional step in viral trafficking, may lead to new treatments for this ubiquitous virus.

Entry of Kaposi's Sarcoma-Associated Herpesvirus Requires Focal Adhesion Kinase (FAK)

Kaposi's sarcoma-associated herpesvirus (KSHV) is the first herpesvirus shown to interact with integrins. Within minutes of its binding to target cells, KSHV activates several integrin-dependent signaling molecules, including FAK, Src, PI-3K, RhoGTPases, PKC-ζ, MEK, and ERK1/2. Krishnan et al. (p. 1167–1180) demonstrate that FAK plays a critical role in KSHV DNA internalization. These data further support the hypothesis that via its interactions with cell-surface receptors, KSHV manipulates cellular signal-transduction pathways for its entry, movement in the cytoplasm, and establishment of infection.

Efficient Adenovirus Production Requires Viral miRNAs

Adenovirus virus-associated I (VAI) RNAs are 160-nucleotide RNA hairpins that block PKR activation in infected cells. Aparicio et al. (p. 1376–1384) provide evidence that VAI RNAs also are processed to form small RNAs that interact with the cellular silencing machinery and allow efficient virus production. These adenovirus miRNAs are suggested to control the expression of cellular or viral genes involved in adenovirus viability. Thus, animal viruses could use the cellular silencing machinery to control gene expression in infected cells.

Insights into Coronavirus Assembly

Coronaviruses assemble on intracellular membranes through a series of membrane protein interactions. Thorp et al. (p. 1280–1289) demonstrate that efficient spike glycoprotein assembly requires posttranslationally added palmitic acids. This

work reveals a novel role for palmitates in generating assembly-competent glycoproteins and underscores the importance of lipid adducts in enveloped virus infectivity.

Antibodies against a Nonstructural Protein Protect against West Nile Virus

Even though not contained in the virion, immunization with flavivirus nonstructural protein 1 (NS1) elicits a protective antibody response through poorly defined mechanisms. Chung et al. (p. 1340–1351) provide new mechanistic evidence about how anti-NS1 antibodies control flavivirus infection. Moreover, they suggest a therapeutic utility of anti-NS1 antibodies as passive transfer even 4 days after inoculation with a lethal West Nile virus strain. By performing studies using complement and Fc γ receptor-deficient mice, the authors demonstrate that anti-NS1 antibodies mapping to distinct protein regions protect against infection through independent mechanisms.

Comparative Quantitative Mass Spectrometry of Wild-Type and Mutant Herpesvirus Virions

A common strategy to elucidate functions of viral proteins is the analysis of specific gene deletion mutants. In an exemplary study on the alphaherpesvirus pseudorabies virus, Michael et al. (p. 1332–1339) present a generally applicable approach to assess qualitative and quantitative changes in protein patterns of mutant virus particles. Using metabolic stable isotope labeling and mass spectrometry, specific alterations in the composition of mutant virions beyond the loss of the targeted gene product were observed that shed new light on the network of protein-protein interactions within the herpesvirus virion.